SUPPORTING INFORMATION

Impurity Retention and Pharmaceutical Solid Solutions: Visualizing the Effect of Impurities on Dissolution and Growth using Dyed Crystals

Anne Nong,[a] Claire Schleper,[a] Abigail Martin,[a] Mitchell Paolello,[a] Fredrik L. Nordstrom [b] and Gerard Capellades*[a]

[a]*Department of Chemical Engineering, Rowan University, Glassboro, New Jersey 08028, United States*

[b]*Material & Analytical Sciences, Boehringer-Ingelheim, Ridgefield, Connecticut 06877, United States*

***Corresponding author e-mail:** capellades@rowan.edu

Image Analysis of Dissolving Crystals

In the manuscript, image analysis was used to identify the relative rates at which product and dye were leaving the crystal during dissolution tests in water. Because dye contents in the crystal and especially in solution at these levels are too small and nearly impossible to quantify, a more accurate approximation was obtained on the basis of projected 2D surface area (dyed vs colorless).

Fig. S1, analogous to the manuscript's Fig. 5, shows examples of an acetaminophen – sulforhodamine B (ACM-SB) crystal as the dissolution test progresses. Note that, as the crystal gets smaller, the picture is further zoomed in to better identify dyed regions. Here, analysis of crystal area would require a consistent scale between magnifications: this was accomplished by using the mesh size on top of which the crystal is sitting. Here, the scale of each image was normalized using the distance in four consecutive mesh gaps, taken near the center of the image and outside (but near) the crystal, where linearity is not distorted by the basket's curvature and by the effect of the crystal's refractive index.

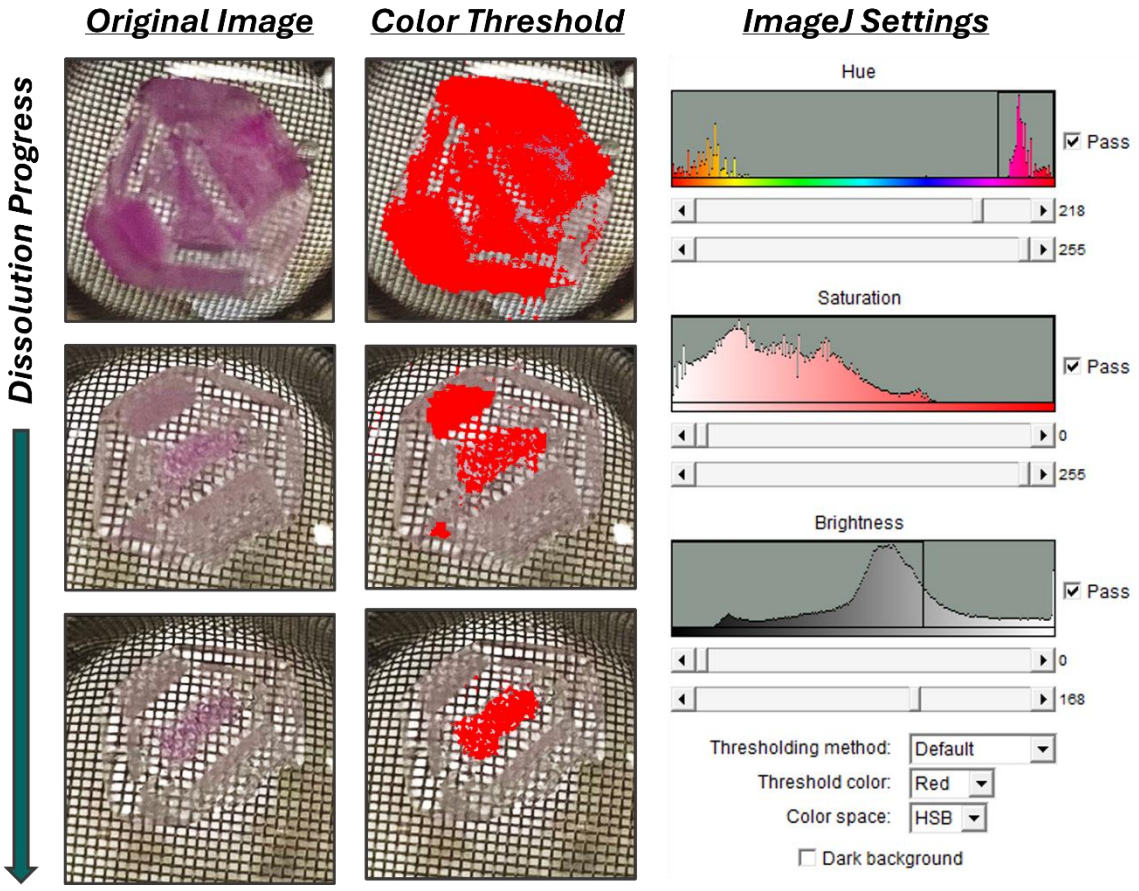

Fig. S1 *Examples of a dissolving ACM-SB crystal analyzed with the color thresholding function of ImageJ. Specific software settings are provided in the figure.*

Once the scales for all images are normalized, two areas are measured: (1) that of the full crystal, by drawing a shape around its contour and asking the software to provide a surface area, and (2) that of the stained areas of the crystal, by using the color thresholding function around the same contour. Settings for color thresholding were manually adjusted and kept constant between images, following the values in Fig. S1. Once both areas are known, their reduction over time can be calculated as equations S1 and S2, and plotted to generate the manuscript's Fig. 5.

$$Dissolution\ Progress\ (\%) = \frac{Starting\ Area - Current\ Area}{Starting\ Area} 100 \quad \text{(S1)}$$

$$Dye\ Loss\ Progress\ (\%) = \frac{Starting\ Dyed\ Area - Current\ Dyed\ Area}{Starting\ Dyed\ Area} 100 \quad \text{(S2)}$$

The same procedure was followed for the analysis of potassium sulfate – acid fuchsin (K_2SO_4-AF) crystals. Specific examples and ImageJ settings are provided in Fig. S2.

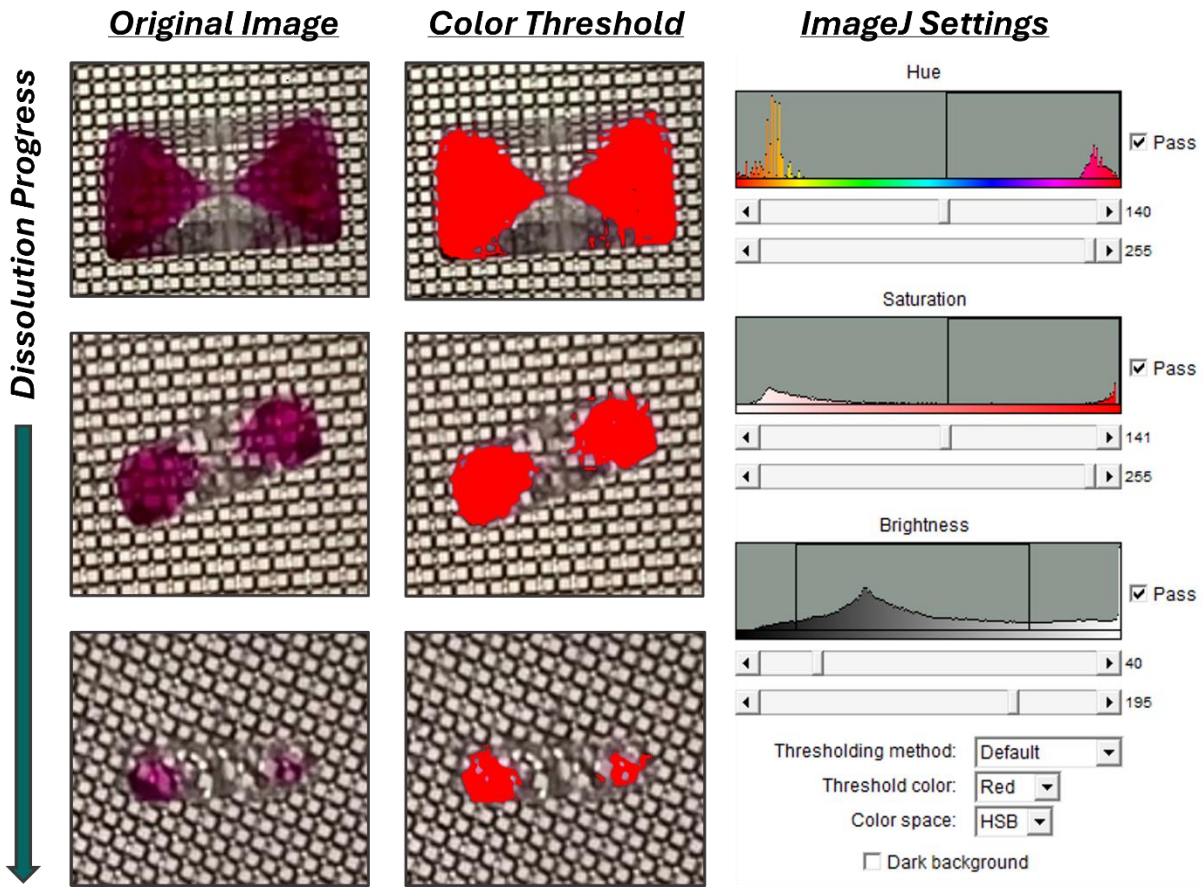

Fig. S2 *Examples of a dissolving K_2SO_4-AF crystal analyzed with the color thresholding function of ImageJ. Specific software settings are provided in the figure.*

When looking at the hues shown in Figs. S1 and S2, note that there are two very distinct regions in an image: one at high hue values (220-255) containing reds and purples, and another at low hue values (0-50) containing organges and yellows. However, the only dyes present in the images are the red/purple SB and AF. The orange hues actually come from the color of the mesh where the crystal is suspended. For this reason, it was not possible to accurately analyze the orange acetaminophen-curcumin (ACM-CUR) crystals without incurring in significant changes in settings and significant bias in the selection of stained areas. An example of the color thresholding attempts for this system is provided in Fig. S3.

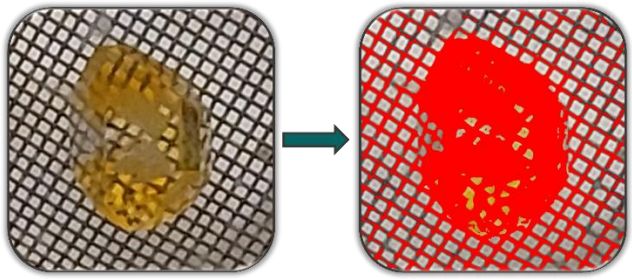

Fig. S3 *Color thresholding attempt for the ACM-CUR system, showing the overlap between hues in the crystal and in the mesh and the potential errors to be incurred due to the mesh contributions to the stained area.*

Change in Morphology During Dissolution

To better visualize the change in morphology for the dissolving crystals, Fig. S4 includes overlays of the 2D crystal morphologies (dimensions approximately adjusted) during the dissolution experiments shown in Figs. 4, 5, and 6 in the manuscript.

Fig. S4 *Overlay of the crystal morphology changes during the dissolution experiments. For ACM-CUR, lines represent the state of the crystal after 2 min, 30 min, 55 min, and 64 min. For ACM-SB, lines represent the state of the crystal after 0 h, 1 h, 3 h, and 5.5 h. For K_2SO_4-AF, lines represent the state of the crystal after 0 min, 5 min, 13 min, and 17 min.*

Ternary Phase Diagram for ACM-AF

While fully mapping the ternary equilibrium of these systems was beyond the objectives of this work, and hindered by the lack of accurate measurements of solid-state purity at these levels, one can use the data gathered for Fig. 10 to generate an approximate ternary phase diagram for ACM-AF. Here, note that because the solid-state miscibilities are so low (ppm levels), the diagram would look very similar to one for immiscible solids.

The pure product solubilities for ACM and AF were 12.8 g/L and 141 g/L, respectively. These values correspond to mole fractions of 0.15% and 0.50% in their respective saturated solutions. The invariant point contains appr. 23 g/L ACM and 160 g/L AF, corresponding to mole fractions of 0.33% for ACM, 0.58% for AF, and 99.09% water. Data for Fig. 10 was collected for solvent fractions below the invariant, with a total solutes concentration of 250 mg/g water. For the system containing only ACM and water, this corresponds to a total water mole fraction of 96.18%. For AF in water, this is 98.99% water. In essence, the mass fractions during the analysis in Fig. 10 were constant, but that is not the case for the mole fractions.

Fig. S5 shows an approximated ternary phase diagram for ACM-AF, utilizing data from Fig. 10 and the knowledge that solid-state miscibilities are near zero. The line in magenta represents the conditions tested in Fig. 10, for which the observed boost in solubilities from pure solutions to the invariant is presented in the blue lines.

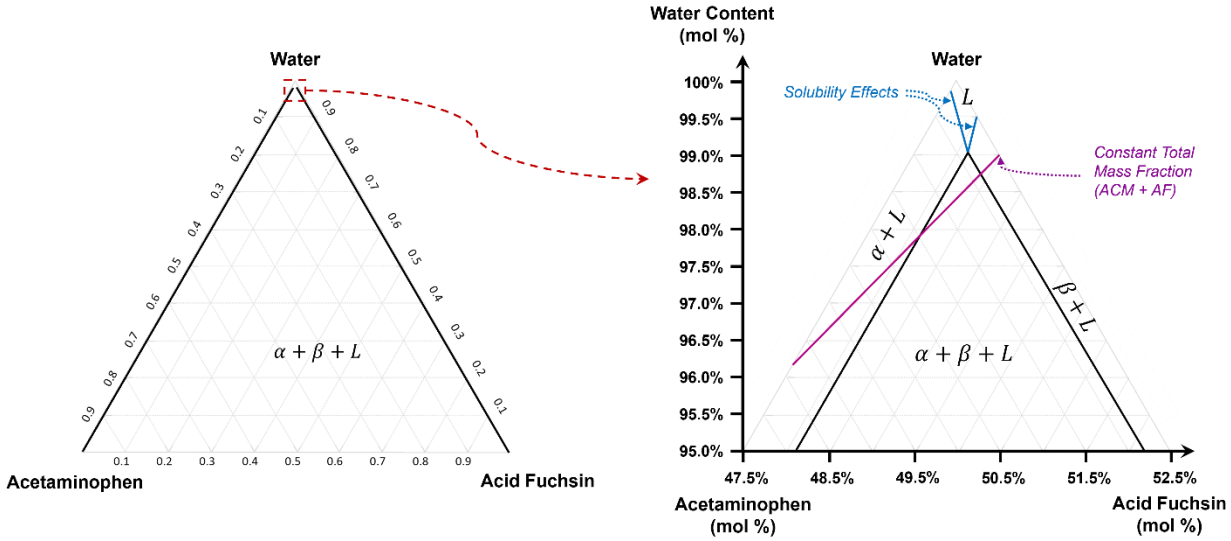

Fig. S5 *Approximate ternary phase diagram for ACM-AF, zoomed in to visualize the region investigated in the manuscript's Fig. 10. Sample conditions followed the magenta line, while solubility reads follow the blue lines. The tilt is due to the conversion from a constant solvent mass fraction to a varying mole fraction (owing to the different molar masses of ACM and AF).*

Note that this works under the assumption that no other impurities were present in those experiments, which is not fully accurate for the AF raw material purity.